





Article

Micro-Siting of Wind Turbines in an Optimal Wind Farm Area Using Teaching–Learning-Based Optimization Technique

Muhammad Nabeel Hussain ¹ , Nadeem Shaukat ^{2,3}, Ammar Ahmad ², Muhammad Abid ^{4,5}, Abrar Hashmi ⁶ , Zohreh Rajabi ⁷  and Muhammad Atiq Ur Rehman Tariq ^{7,8,*} 

- ¹ Department of Mechanical Engineering, Pakistan Institute of Engineering & Applied Sciences, Nilore, Islamabad 45650, Pakistan; nabeel106d@gmail.com
- ² Center for Mathematical Sciences (CMS), Pakistan Institute of Engineering & Applied Sciences, Nilore, Islamabad 46560, Pakistan; drnadeem_shaukat@pieas.edu.pk (N.S.); ammar_nustian@hotmail.com (A.A.)
- ³ Department of Physics and Applied Mathematics (DPAM), Pakistan Institute of Engineering & Applied Sciences, Nilore, Islamabad 45650, Pakistan
- ⁴ Department of Mechanical Engineering, COMSATS University Islamabad, Wah Campus, Wah Cantt 47040, Pakistan; drabid@ciitwah.edu.pk
- ⁵ Interdisciplinary Research Center, COMSATS University Islamabad, Wah Campus, Wah Cantt 47040, Pakistan
- ⁶ Department of Electrical Engineering, Capital University and Technology, Islamabad 45750, Pakistan; abrarhashmi313@gmail.com
- ⁷ Institute for Sustainable Industries & Liveable Cities, Victoria University, P.O. Box 14428, Melbourne, VIC 8001, Australia; zohreh.rajabi@live.vu.edu.au
- ⁸ College of Engineering, IT & Environment, Charles Darwin University, Darwin, NT 0810, Australia
- * Correspondence: atiq.tariq@yahoo.com



Citation: Hussain, M.N.; Shaukat, N.; Ahmad, A.; Abid, M.; Hashmi, A.; Rajabi, Z.; Tariq, M.A.U.R. Micro-Siting of Wind Turbines in an Optimal Wind Farm Area Using Teaching–Learning-Based Optimization Technique. *Sustainability* **2022**, *14*, 8846. <https://doi.org/10.3390/su14148846>

Academic Editors: Désiré Rasolomampionona and Klos Mariusz

Received: 31 May 2022

Accepted: 14 July 2022

Published: 19 July 2022

Publisher's Note: MDPI stays neutral with regard to jurisdictional claims in published maps and institutional affiliations.



Copyright: © 2022 by the authors. Licensee MDPI, Basel, Switzerland. This article is an open access article distributed under the terms and conditions of the Creative Commons Attribution (CC BY) license (<https://creativecommons.org/licenses/by/4.0/>).

Abstract: Nowadays, wind energy is receiving considerable attention due to its availability, low cost, and environment-friendly operation. Wind turbines are rarely placed individually but rather in the form of a wind farm with a group of several wind turbines. The purpose of this research is to perform studies on wind turbine farms in order to find the best distribution for wind turbines that maximizes the produced power, hence minimizing the wind farm area. Wind Farm Area Optimization (WFAO) is performed for optimal placement of wind turbines using elitist teaching–learning-based optimization (ETLBO) techniques. Three different scenarios of wind (first is fixed wind direction and constant speed, second is variable wind direction and constant speed, and third is variable wind direction and variable speed) are considered to find the optimal number of turbines and turbine positioning in a minimized squared land area that maximizes the power production while minimizing the total cost. Other research carried out in the past was to find the optimal placement of the wind turbines in a fixed squared land area of 2 km × 2 km. In the present study, WFAO–ETLBO algorithm has been implemented to get the optimal land area for the placement of the same number of turbines used in the past research. For Case 1, there is a significant reduction in land area by approximately 30.75%, 45.25%, and 51.75% for each wind scenario, respectively. For Case 2, the reductions in land area for three different wind scenarios are respectively 30.75%, 7.2%, and 7.2%. For Case 3, there is a reduction of 7.2% in land area for each wind scenario. It has been observed that the results obtained by the WFAO–ETLBO algorithm with a significant reduction in the land area along with optimal placement of wind turbines are better than the results obtained from the wind turbines placement in the fixed land area of 2 km × 2 km.

Keywords: wind turbine; micro-siting; wind farms; teaching–learning-based optimization; Jensen's wake modeling

1. Introduction

The computational intelligence techniques have been extensively used by numerous studies for wind farm layout optimization purposes. Most of the contributions include gradient-free methods, and most of them use soft computing. Soft computing includes

artificially intelligent techniques which are stochastic in nature and metaheuristic. The effectiveness and the comparison studies of these soft computing techniques have been shown in different studies by different researchers for the positioning optimization of wind turbines. In order to place a large number of wind turbines in the wind farm, it is needed to find the optimal placement of these turbines to get the maximum expected power production at a minimizing cost.

Several pieces of research have been performed to optimize the placement of wind turbines [1,2]. Mosetti et al. employed the genetic algorithm to find the optimal wind turbine placement in wind farms [1]. Grady et al. challenged the results of Mosetti et al. and claimed that the results produced by Mosetti et al. were not optimum [2]. Mittal et al. also employed the genetic algorithm to find the optimal placement of wind turbines in wind farms [3,4]. They produced results for three different scenarios for fixed wind direction at constant speed but having a change in direction and variable wind speed and variable direction with some preferred directions, respectively. They used Jensen's analytical wake model for modeling the wake effect, and their main objective was to minimize the value of cost per unit of power [5]. They recommended that a sufficient number of generations were not considered to arrive up to the optimum point. Rabia et al. proposed a method for wind farm layout optimization by using definite point selection and a genetic algorithm that can improve the wind farm's output power by changing the wind farm's dimensions with an area size of $2 \text{ km} \times 2 \text{ km}$ [6]. They rotated the square-shaped wind farm by 45 degrees towards the uniform direction of the wind, and a definite point selection criterion was set in order to face the upstream wind. These researches proposed the optimal number of turbines along with their optimal placements in the wind farm of the fixed square land area of $2 \text{ km} \times 2 \text{ km}$. Many have used gradient-based wind farm layout optimization solvers consisting of combinatorial optimization and sequential linear or sequential quadratic programming [7–9]. Until now, a number of contributions through the implementation of intelligent evolutionary techniques have been made toward the optimal placement of wind turbines in a given land area of a wind farm. The different sub-categories of the soft computing techniques include Genetic algorithms with different hub heights [10], a new mathematical programming approach to optimize wind farm layouts [11], viral-based optimization algorithm [12], particle swarm optimization technique [13], mixed integer linear programming [14], multi-population genetic algorithm [15], colony algorithm [16], random and local search algorithm [17–19], and simulated annealing [20]. Optimizing the layout of wind farm turbines using genetic algorithms has been performed in Tehran province [21]. A new approach for power prediction has been implemented to analytically model wind farms [22].

In order to maximize the wind energy capture, a model for wind turbine placement based on the wind distribution has already been proposed [23]. The model calculated wake loss based on wind turbine locations and wind direction. A multi-objective evolutionary strategy algorithm has been developed to solve the transformed bi-criteria optimization problem, which maximizes the expected energy output, as well as minimizes the constraint violations. A proposed wind farm layout upgrades by adding different (in type and/or hub height) commercial turbines to an existing farm have been introduced and optimized. Three proposed upgraded layouts have been considered: internal grid, external grid, and external unstructured. A genetic algorithm has been used for the optimization purpose, and the manufacturer's power curve and a general representation for thrust coefficient were used in power and wake calculations, respectively. A simple field-based model has been implemented while considering both offshore and onshore conditions [24,25]. WFLO problem that gives total freedom to the wind farm area shape has been presented for the first time while considering that increasing the degrees of freedom in the decision space can lead to more efficient solutions in an optimization problem. Multi-objective optimization with the power output (PO) and the electricity cable length (CL) as objective functions in Horns Rev I (Denmark) via 13 different genetic algorithms: a traditionally used algorithm, a newly developed algorithm, and 11 hybridizations resulting from the

two has been presented. Turbine wakes and their interactions in the wind farm have been computed through the in-house Gaussian wake model [26]. A distributed genetic algorithm has been deployed to study the wind turbine's layout in order to improve the wake effect [27]. The optimal arrangement of the wind farm and the best values for the hubs of its wind turbines in Manjil, Iran, have been proposed. Jensen's wake model has been used by considering wind regimes and geographic data of the considered area with electricity generation costs along with the objective function, based on the Mosetti et al. cost function, by implementing the particle swarm optimization (PSO) algorithm [28]. A software design tool has been developed to examine the significance of wind turbine's layouts (M, straight and arch shapes) and spacing on the final energy yield with five times rotor diameter distance between each turbine has been simulated and has resulted in 22.75, 22.87 and 21.997 GWh/year for the M shape, Straight line and Arch shape, respectively [29].

The relocation of several wind turbines has been transformed into a single-player reinforcement learning problem, which is further handled by Monte-Carlo Tree Search integrated into the evolutionary algorithm, improving the exploitation potential in the adaptive genetic algorithm. The enhanced algorithmic exploitation used on the wind farm in New Jersey resulted in a significant improvement and better performance when compared to benchmark algorithms [30]. A novel coupling approach has been used to optimize the layout of wind farms while taking into account inhomogeneous wave loads on monopile-supported wind turbines. The basic objective is to position every turbine in the best possible way, minimizing the wind farm's overall wave load while maintaining a good annual energy output [31]. The wake model, optimization technique, and objective function, respectively, have been the PARK approach, genetic algorithm, and Levelized Cost of Electricity (LCOE). A total of 36 Cartesian wind farm grids with various resolutions were taken into account in order to find the best wind farm layouts. Following the identification of the ideal layout, an economic analysis was carried out to look at the effects of governmental incentives on the viability of the ideal wind farm [32]. Recent experimental, computational, and theoretical research initiatives that have helped advance our comprehension and capacity to foresee the interactions of the turbulent atmospheric boundary layer (ABL) flow with wind turbines and wind farms have been reviewed [33]. The gradients required for optimization have been discovered by solving the adjoint equations of the flow model at a cost that is independent of the number of control variables, enabling the optimization of huge wind farms with numerous turbine sites. For idealized test situations, gradient-based optimization of wind turbine placement has been shown. These instances show new optimization heuristics, including rotational symmetry, local speedups, and nonlinear wake curvature effects. On more complicated wind rise shapes, layout optimization has also shown to be effective. This includes a full annual energy production (AEP) layout optimization over 36 input directions and five wind speed bins [34]. A novel approach for the optimization of wind farm layouts has been published that enables the use of CFD models to precisely replicate wake effects and terrain-induced flow characteristics. This methodology uses a gradient-based algorithm and an adjoint method for gradient computations. In contrast to other studies, this methodology has a general formulation to be used for a variety of wind farm layouts, wind resource distributions, and topographic conditions. Benefits of an ideal wind farm design that makes use of CFD models are shown for both idealized and practical scenarios, where it is possible to achieve notable increases in annual energy production by strategically placing turbines on difficult terrain [35]. By using an undirected graph to model the quadratic integer formulation of the discretized layout design problem, a novel method has been developed to quickly produce approximative optimal layouts to support infrastructure design decisions. This method effectively captures the spatial dependencies of the design parameters caused by wake interactions. The probabilistic inference on the undirected graph uses sequential tree-reweighted message forwarding to approximate the turbine siting. By comparing the method's performance to a cutting-edge branch and cut algorithm at various wind regime complexity levels and wind farm discretization resolutions, its

efficacy has been evaluated [36]. In order to determine the best wind farm dimensions where the most area may face the free stream velocity, an area rotation method has been created. The placement of the turbines has been suggested using a novel technique known as definite point selection (DPS), which may also be used to locate the wind farm's zero wake effect spots. DPS requires a minimum distance between neighboring turbines for operation safety [37].

Based on the thorough literature analysis provided in Section 1, prior studies have focused on the issues with wind farm layout optimization. However, the present study focuses on the following objectives:

- Minimization of the land area of wind farm
- Maximization of the power production
- Minimization of the total cost

This study is novel because it uses a teaching learning-based optimization technique to offer a new optimization function for wind farm area optimization. The importance of the issue is to draw attention to the economic benefits of area reduction before building the wind turbines in a wind farm with a smaller footprint. The elitist teaching–learning–based optimization (ETLBO) algorithm [38–42] is employed to perform wind farm area optimization (WFAO) along with the optimal placement of the wind turbines. The WFAO–ETLBO algorithm is used due to its certain advantages over other optimization techniques. The Optimization procedure starts with the input of basic parameters of the wind turbine, such as wind turbine specifications, total area and specific dimensions of the wind turbine, wind scenarios, terrain characteristics, total number of wind turbines to be installed in the wind farm. The area or dimensions of a wind farm are strongly influenced by the available wind scenarios and terrain characteristics. These are value-added outcomes that have not been identified so far. When using the proposed method, wind farms have been selected to use the minimum width in the wind speed direction to achieve maximum power generation at the lowest cost. The minimized area is found for the optimal placement of the turbines and performed for three different wind scenarios having fixed wind direction and constant speed, variable wind direction, and constant speed and variable wind direction and variable speed, respectively, to achieve maximum energy production at the minimum total cost. Results of WFAO–ETLBO are compared with the other studies and proposed that the significant reduction in area can be made to place the same number of turbines with comparable results obtained by other studies. It is seen that the results are more accurate and advantageous than the others and are discussed in detail in the subsequent sections.

2. Materials and Methods

2.1. Jensen's Wake Effect Modeling

Jensen's wake model to find the optimal wind farm layout design in a minimized land area is taken into consideration in the present study because previous studies have extensively utilized the current wake model. Here, it is considered to be appropriate for validation purpose. It was initially proposed by Mosetti et al. [2] and Grady et al. [3]. The assumptions made in the initial studies are still being used in recent studies. The schematic diagram of Jensen's wake model is shown in Figure 1.

Where $\alpha = \tan \frac{\theta}{2}$, $\theta = 2 \tan^{-1} 0.09437 = 10.787$ and x is the wind downstream distance. As wind turbines are to be placed at the origin of each cell, so x can have only these values: $x = 5d, 10d, 15d$ is to $45d$, where d is the distance between 1st and 10th turbine (if there is turbine)

So, we will be only evaluating the $\frac{u}{u_0}$ on above values of x .

Wake effect behind a turbine

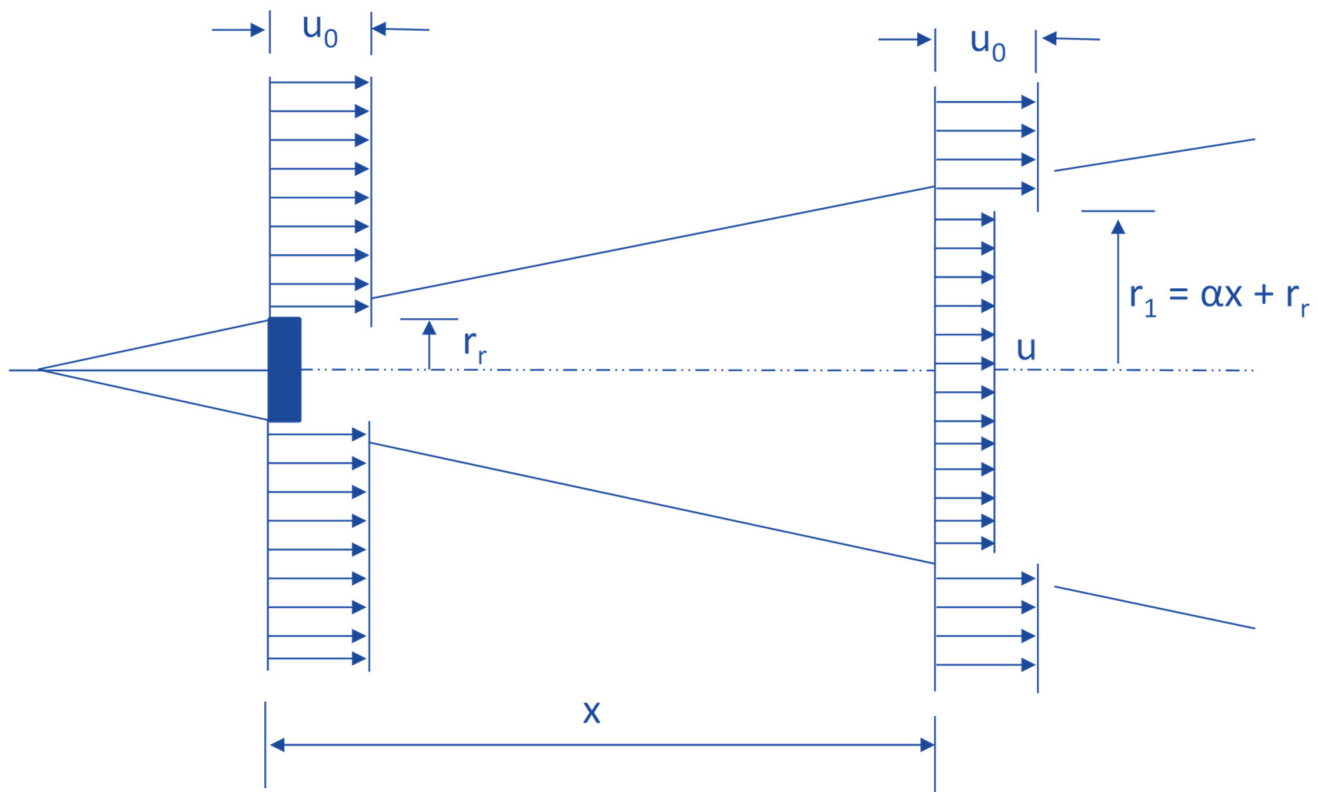


Figure 1. Wake effect model of wind turbine.

Expression for calculating the velocity of air behind the turbine after it has passed through the turbine is given by N. O. Jensen's wake model [4] in Equation (1),

$$\frac{u}{u_0} = \left[1 - \frac{2a}{\left(1 + \alpha \left(\frac{x}{r_1} \right) \right)^2} \right] \quad (1)$$

where,

$$a = \frac{\text{upstream velocity} - \text{velocity just behind the rotor}}{\text{upstream velocity}}$$

This model predicts the velocity of air behind the turbine rotor at any distance x from the turbine. This model predicts that the velocity of air is the smallest just behind the rotor, and it starts recovering its velocity as it moves away from turbines. At a large distance from turbines, velocity fully recovers and becomes equal to the free stream velocity [10]. A change in velocity with distance is plotted in Figure 2.

For calculating the velocity of air at a turbine experiencing multiple wakes, the resultant velocity is calculated by assuming that sum of kinetic energy (K.E.) deficit at the turbine being considered is equal to the K.E. deficit of mixed wake [11].

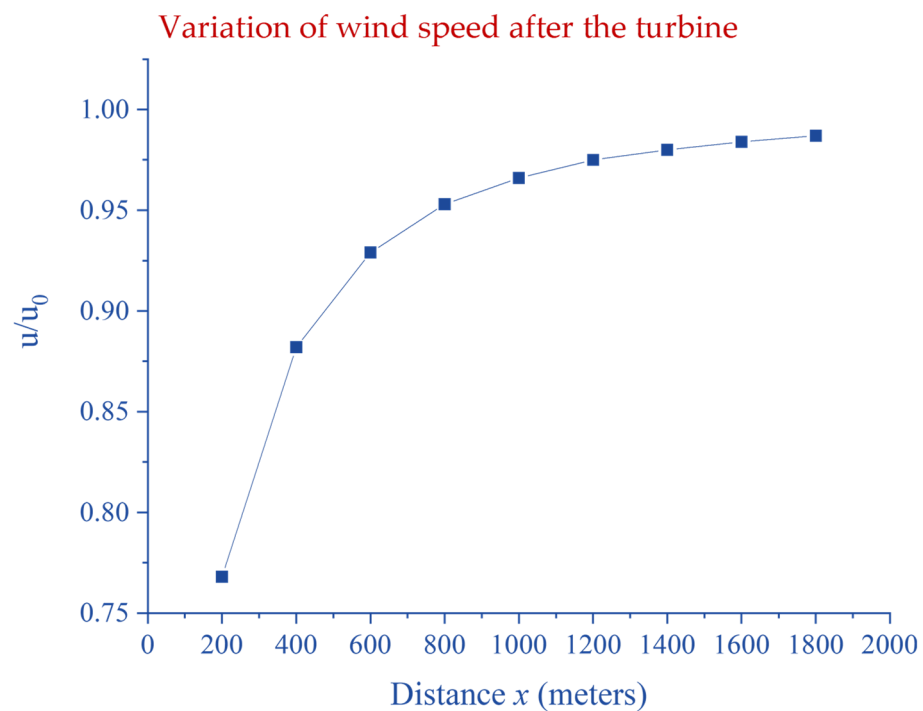


Figure 2. Variation of wind speed after the turbine with respect to distance x .

2.2. Fitness Evaluation

2.2.1. Wind Farm Cost Estimation

Mosetti et al. presented an empirical relation to calculate cost/year dependent on number of turbines in Equation (2a);

$$\text{cost of } N \text{ turbines} = N \left(\frac{2}{3} + \frac{1}{3} e^{-0.00174N^2} \right) \quad (2a)$$

They assumed that above-modeled cost/year of a single turbine is one with a maximum reduction in the cost of $1/3$ for each additional turbine.

$$\lim_{N \rightarrow \infty} \left(\frac{2}{3} + \frac{1}{3} e^{-0.00174N^2} \right) = \frac{2}{3} \quad (2b)$$

So, if the cost for each turbine is 1. For large number of turbines, cost reduces from 1 to $\frac{2}{3}$ i.e., $1 - \frac{2}{3} = \frac{1}{3}$ cost reduction can be performed for each additional turbine [11,12].

2.2.2. Wind Farm Power Estimation

Power for wind turbine is given in Equation (3a,3b);

$$P = \frac{1}{2} \dot{m} u^2 = \frac{1}{2} (\rho A u) u^2 \quad (3a)$$

$$P = \frac{1}{2} \rho A u^3 \quad (3b)$$

ρ is considered to be constant here. ρ is calculated according to general gas equation at fixed atmospheric conditions given by Equation (4);

$$\rho = \frac{P}{RT} \quad (4)$$

$$\rho = \frac{101325}{287 * 293} = 1.2 \text{ kgm}^{-3}$$

Using Equation (4), the ideal power P_{ideal} can be estimated as;

$$P_{\text{ideal}} = \frac{1}{2} * 1.2 * \frac{\pi}{4} * 40^2 * u^3 = 754u^3 \text{ watts} \quad (5)$$

Assuming efficiency of turbine to be 40%. The actual power P produced is calculated by using Equation (6a);

$$\text{Efficiency} = \frac{P}{P_{\text{ideal}}} = 1.2 \text{ kgm}^{-3} \quad (6a)$$

$$P = 0.4 * \frac{754}{1000} u^3 \text{ KW} = 0.3(u_{\text{wmwe}})^3 \text{ KW} \quad (6b)$$

where u_{wmwe} is the velocity of the turbine with multiple wake effect. Thus, Equation (6b) can be written as;

$$P \propto (u_{\text{wmwe}})^3 \quad (6c)$$

Equation (6c) shows that power produced by the turbine is directly proportional to the cube of velocity [13,23].

2.2.3. Evaluation of Fitness Function

The main objective of the present study is the generation of optimal layout of the turbines at such positions in a minimized wind farm land area so as to produce maximum power while minimizing the cost. Therefore, the objective of the layout optimization problem can be stated mathematically as;

$$\begin{aligned} \text{objective function} &= \text{minimize} \left(\frac{\text{Total Cost}}{\text{Total Power}} \times \text{Area} \right) \\ &= \text{minimize} \left(\frac{N \left(\frac{2}{3} + \frac{1}{3} e^{-0.00174N^2} \right)}{0.3(u_{\text{wmwe}})^3} \times xy \right) \end{aligned} \quad (7)$$

where x and y are the lengths and width of the wind farm. In case of square land area; $x = y$.

As in the current study, we are already talking about the economic aspect of the wind farms without considering the available budget in the formulation. There are primarily two types of objective functions used in the optimization formulas in the previous outdated studies (cost per unit power and one over power). They do not, however, have any financial or technological restrictions that might effectively regulate a budget limitation or a turbine number. In the present objective function formulation, the economic aspect is obvious with the consideration of land area.

2.2.4. Calculation of Efficiency

Efficiency of the wind farm is the amount of energy extracted from the total energy of the wind farm without considering the effect of wake. It should not be confused with the efficiency of the wind turbine. It estimates the actual power produced from the wind farm compared to the power produced from the same number of turbines. The efficiency of the turbine is considered as the aerodynamic efficiency of the rotor or blade of the turbine. It is a measure of the energy extracted from the wind through blades. Mathematically, efficiency (η) of the wind farm installed with N number of turbines is estimated by the ratio of the total power with multiple wake effects, i.e., $P_{\text{tot,wmwe}}$ to the total power without wake effects, i.e., $P_{\text{tot,wowe}}$;

$$\eta = \frac{P_{\text{tot,wmwe}}}{P_{\text{tot,wowe}}} \quad (8)$$

In case of Scenario-II, with constant speed and variable direction, the formulations for the total power with multiple wake effects (P_{wmwe}) and without considering wake effects (P_{wowe}) are respectively given as;

$$P_{wmwe} = \sum_{k=1}^{N_T} \sum_{\theta_i=1}^{36} 0.3 * f_{(\theta_{i-1}) * 10, j} * u_0^3 * \left(\frac{v}{u}\right)_k^3; \theta_i = 0, 10, 20 \dots 350 \quad (9)$$

$$P_{wowe} = N_T * \sum_{\theta_i=1}^{36} 0.3 * f_{(\theta_{i-1}) * 10, j} * u_0^3; \theta_i = 0, 10, 20 \dots 350 \quad (10a)$$

where;

$$f_0 = f_{10} = f_{20} = \dots = f_{350} = \frac{1}{36} \text{ (wind occurrence probability @ each angle)}$$

$$\sum_{\theta_i=1}^{36} f_{(\theta_{i-1}) * 10, j} = 1$$

So,

$$P_{wowe} = N_T * 0.3 * u_0^3 \quad (10b)$$

While in case of Scenario-III, with variable speed and variable direction, the formulations for the total power with multiple wake effects (P_{wmwe}) and without considering wake effects (P_{wowe}) are respectively given as;

$$P_{wmwe} = \sum_{k=1}^{N_T} \sum_j \sum_{\theta_i=1}^{36} 0.3 * f_{(\theta_{i-1}) * 10, j} * u_j^3 * \left(\frac{v}{u}\right)_k^3 \quad (11)$$

$$P_{wowe} = N_T * \sum_j \sum_{\theta_i=1}^{36} 0.3 * f_{(\theta_{i-1}) * 10, j} * u_j^3 \quad (12)$$

where;

$$\theta_i = 0, 10, 20 \dots 350$$

$$j = 8, 12, 17 \text{ (wind speed values)}$$

$$k = 1, 2, 3 \dots N_T \text{ (Number of Turbines)}.$$

2.3. Elitist Teaching–Learning-Based Optimization Algorithm

The problem of wind farm area optimization along with placement optimization is solved using teaching–learning-based optimization technique with elitism. Teaching–Learning-based optimization algorithm (TLBO) is proposed by the Indian researcher R. Venkata Rao [41]. This optimization algorithm mimics the teaching and learning in the environment of classroom to improve the average students of classroom. The whole learning procedure of teacher's and learner's phase will continue until the convergence criteria is met [42]. The pseudo code for the TLBO algorithm with elitism is given in Figure 3 below;

Pseudo-code Teaching-learning-based optimization algorithm

```

1:  Generate initial population of wind farm layouts as initial learners  $L$ 
2:  Calculate the mean of each learner in the population ( $L_{mean}$ )
3:  Compute the fitness value  $f$  of each learner in the population
4:  Identify the best fitness ( $L_{teacher}$ )
5:  Keep assigned number of elite solutions
6:  Generate a new population based on the  $L_{teacher}$ ,  $L_{mean}$  and  $T_F$ .
7:  for  $i = 1 : 1 : \text{No. of learners in the population } L$ 
8:       $T_F = rand[1,2]$ 
9:       $L_i(new) = L_i(old) + rand(i) * (L_{teacher} - T_F * L_{mean})$ 
10:  end for
11:  Update population of learner  $L$  by comparing old population  $L_i(old)$  and new
    population  $L_i(new)$ 
12:  for  $i = 1 : 1 : \text{No. of learners in the population } L$ 
13:      if ( $L_i(old) < L_i(new)$ )
14:           $L_i = L_i(new)$ 
15:      else
16:           $L_i = L_i(old)$ 
17:      end if
18:  end for
19:  Randomly select two learners as  $L_i$  and  $L_j$  from the population and improve their
    fitness.
20:  if ( $f(L_i) < f(L_j)$ )
21:       $L_i(new) = L_i(old) + rand(i) * (L_j - L_i)$ 
22:  else
23:       $L_j(new) = L_j(old) + rand(i) * (L_i - L_j)$ 
24:  end if
25:  Calculate the fitness values  $f(L_i(new))$  and  $f(L_j(new))$ 
26:  Replace the worst solution with the elite solution
27:  Check for termination criteria on the maximum difference between two succes-
    sive iterations;
28:  if ( $\max(|f(L_i(new)) - f(L_{i-1}(new))|; \forall i = 1, 2, 3, \dots, N) < \varepsilon_1$ )
29:      if ( $|f(L_j(new)) - f(L_{j+1}(new))|; \forall i = 1, 2, 3, \dots, N < \varepsilon_2$ )
30:          Reached Stop
31:      else
32:          Go to line 3 and Compute the fitness value  $f$  of each learner in the popu-
            lation
33:      end if
34:  else
35:      Go to line 3 and Compute the fitness value  $f$  of each learner in the population
36:  end if
37:  Return the optimal layout  $L$  with minimum fitness  $f$ 

```

Figure 3. Pseudo-code of the Teaching-learning-based optimization algorithm [40].

2.4. Different Wind Scenarios

2.4.1. Scenario-I: Uni-Directional Wind with the Identical Velocity

In this case, the simplest of all, wind blows from only one direction with constant wind speed of 12 ms^{-1} . In this case, it is easy to find an optimal placement of a certain number of wind turbines in a given land area. As the direction of the wake is also unidirectional, so the maximum number of turbines can be placed in line to get the maximum power output. Most the turbines can be placed at the initial boundary and the end boundary. Rest of the turbines can be placed randomly with the minimum effect of wake. In unidirectional

case, the computational expense will also be very low to find the optimal solution rapidly. Following wind rose shown in Figure 4a shows the frequency distribution for Scenario-I.

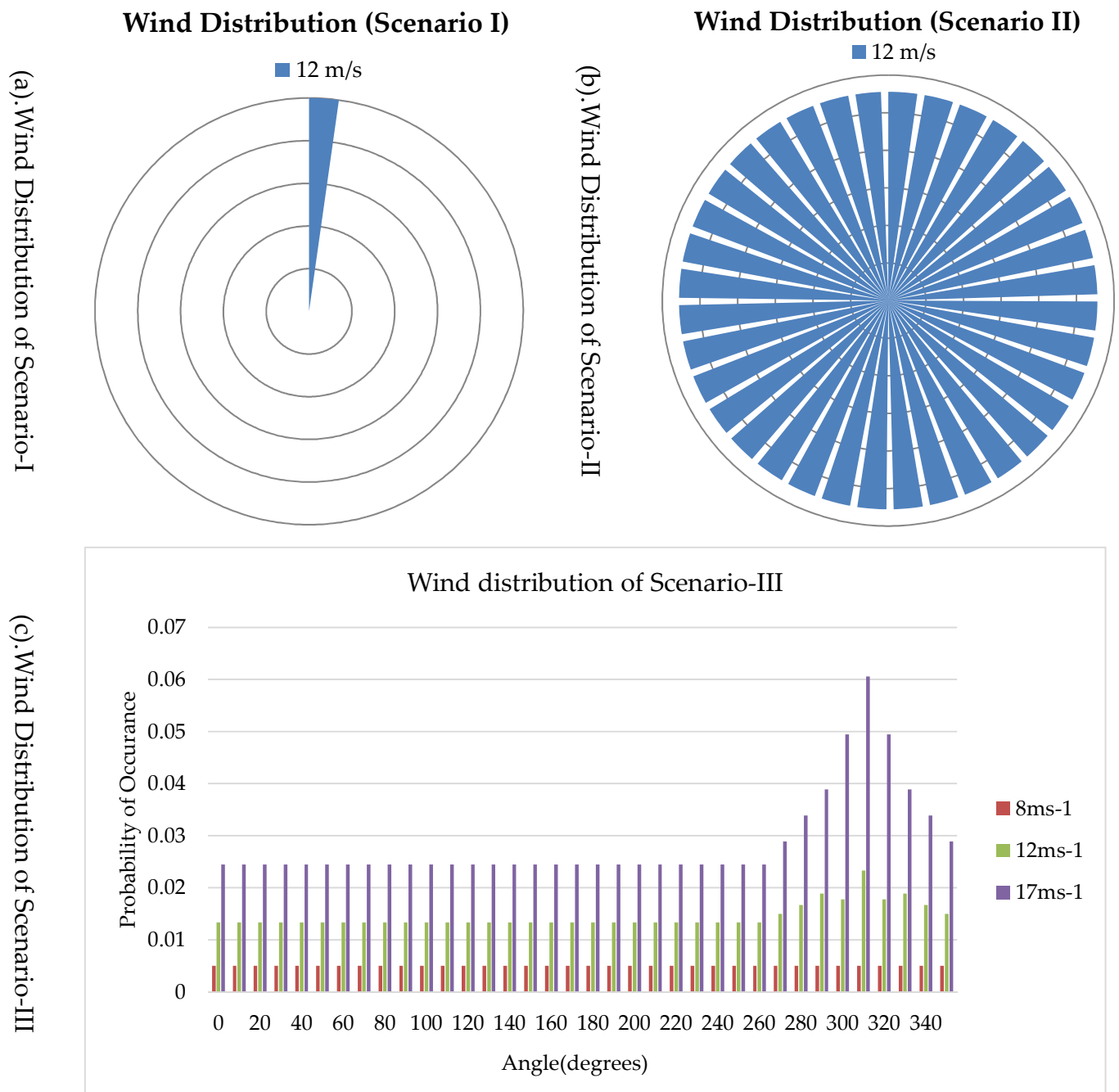


Figure 4. Frequency Distribution for (a) Wind Scenario-I; (b) Wind Scenario-II; (c) Wind Scenario-III.

2.4.2. Scenario-II: Multi-Directional Wind with the Identical Velocity

In this case, wind blows at constant speed, but it may occur from any direction. The circle is divided into 36 segments. Each segment has equal probability of wind occurrence with speed of 12 ms⁻¹. The wind rose shown in Figure 4b shows the frequency distribution for Scenario-II.

2.4.3. Scenario-III: Multi-Directional Wind with Variable Wind Velocity

Third case is relatively a general case. Here three wind speeds of 8 ms⁻¹, 12 ms⁻¹ and 17 ms⁻¹ are considered. These three speeds have different probability of occurrence

from different sides. In real wind scenarios, wind speed does not have fixed value; rather, there are wind speed groups. The wind rose shown in Figure 4c shows the frequency distribution for Scenario-III.

3. Results

Three different wind scenarios are considered to find the optimal area for placement of turbines with the same number of turbines used in previous research and to maximize the expected power production while minimizing the total cost. These scenarios used to test the algorithm are based on the same settings of $2\text{ km} \times 2\text{ km}$ land area, a 60 m hub height, a 40 m radius, a constant thrust coefficient, and three different wind scenarios used by three different researchers [1–3]. The studies of those three different researchers on the same scenarios using a coarse grid with five times rotor diameter (i.e., 200 m) as the center-to-center distance between two adjacent wind turbines and fixed land area are compared with the results obtained from WFAO–ETLBO algorithm. These settings were the need for comparison with previous literature. WFAO–ETLBO produces good results with minimum fitness while producing maximum power and efficiency with a significant reduction in land area as compared to Mosetti et al., Grady et al., and Mittal et al. with less number of iterations as well. The results of all the three studies performed on the same problems considered in this work are discussed in the subsequent sections.

3.1. Case 1 vs. WFAO–ETLBO

The Case 1 considers the results obtained by Mosetti et al. for all the three different scenarios used in this study. Mosetti et al. used 26 turbines in for Scenario-I, 19 turbines for Scenario-II, and 15 turbines for Scenario-III to find the optimal placement of wind turbines in a fixed land area of $2\text{ km} \times 2\text{ km}$. The layout proposed was not symmetrical [1].

WFAO–ETLBO algorithm is used to solve the same scenarios considered by Mosetti et al. with a different number of turbines. Table 1 shows the comparisons of results for all the wind scenarios obtained by Mosetti et al. with those obtained from WFAO–ETLBO with fine grid meshing. The total power produced is 2.07%, 9.74%, and 9.97% lower than those quoted by Mosetti et al. for all the scenarios, respectively. The relative change (R.C.) in efficiency is 2.07%, 9.74%, and 9.26%, respectively, for all the scenarios. From Table 1 it can also be noted that the algorithm is converged in a significantly smaller number of iterations as compared to Mosetti. Thus, the computational expense of WFAO–ETLBO is expressively small in comparison with the soft computing technique used by the previous studies. Figure 5 represents difference plots for each learner to ensure the convergence of the WFAO–ETLBO algorithm and show the convergence of the land area for optimal placement of wind turbines in the case of all the scenarios, respectively. The most optimal layouts generated with fine grid meshing for Scenario-I, Scenario-II, and Scenario-III, respectively, are shown in Figure 6, along with the original layouts proposed by Mosetti et al. The same number of turbines are placed at the optimal locations with a significant reduction of 30.75%, 45.25%, and 51.75% in the land area for Scenario-I, Scenario-II, and Scenario-III, respectively, while producing comparable power for each scenario.

Table 1. Comparisons of results obtained by Mosetti et al. [1] and WFAO–ETLBO.

	Scenario-I		Scenario-II		Scenario-III	
	Mosetti et al.	WFAO–ETLBO	Mosetti et al.	WFAO–ETLBO	Mosetti et al.	WFAO–ETLBO
Number of turbines	26	26	19	19	15	15
Number of individuals	200	100	200	100	200	100
Fitness value	0.001619	0.0015868	0.0017371	0.0019232	0.00099405	0.0010977
Total Power (KW/year) (R.C. (%))	12,352	12,607.9 (2.07)	9244	8343.51 (9.74)	13,460	12,116.91 (9.97)
Efficiency (%) (R.C. (%))	91.65	93.54 (2.07)	93.851	84.71 (9.74)	94.62	85.85 (9.26)
Converged number of iterations	400	75	350	15	400	15
Area Used (m)	2000 × 2000	1385 × 1385	2000 × 2000	1095 × 1095	2000 × 2000	966 × 966
% Reduction in Area	~	30.75	~	45.25	~	51.75
Simulation Time (s)	Not reported	480.2	Not reported	708.7	Not reported	534.5

Difference plot for each learner

Convergence plot for optimal length

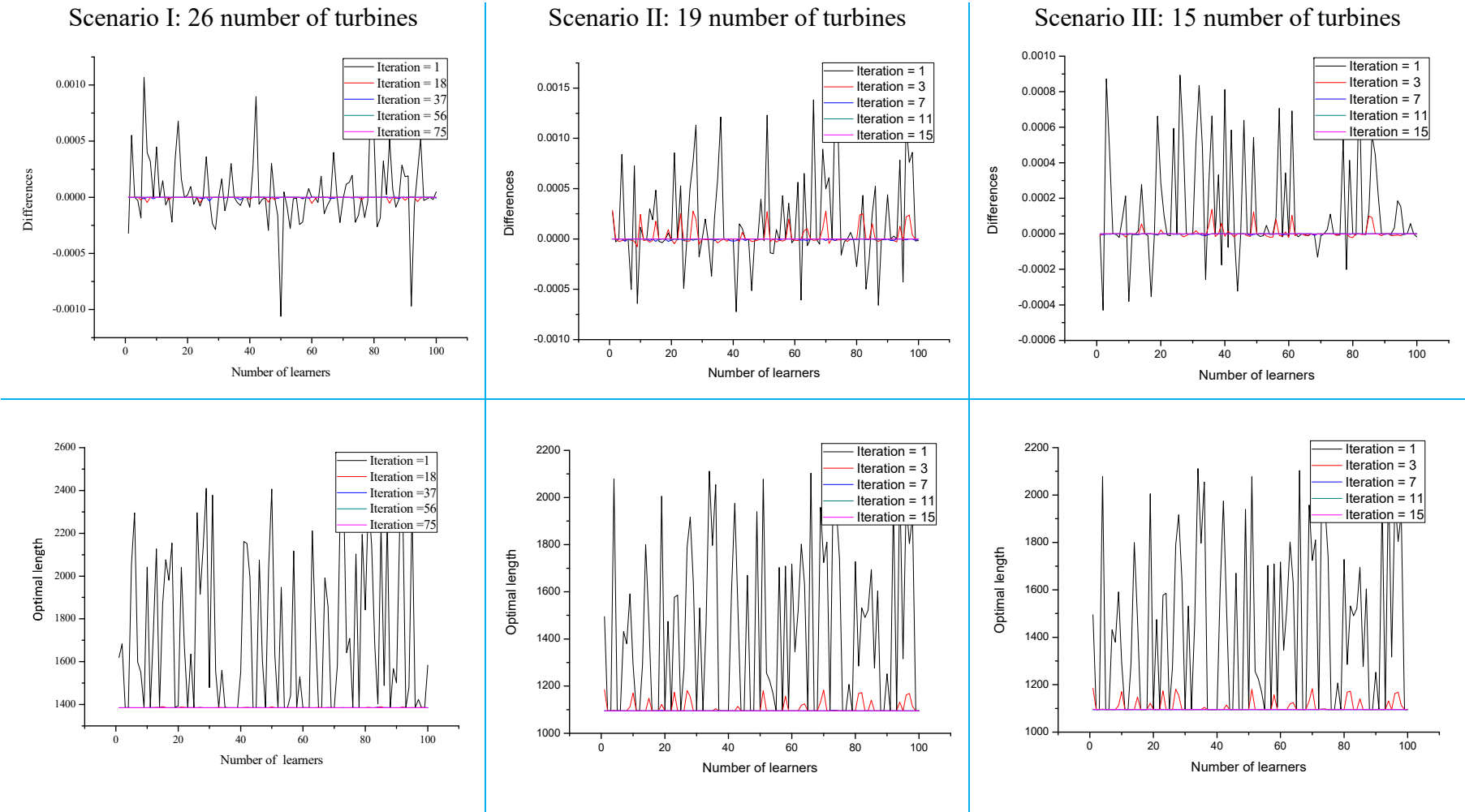


Figure 5. Difference plots for each learner and convergence plots for optimal length for all Scenarios using WFAO-ETLBO.

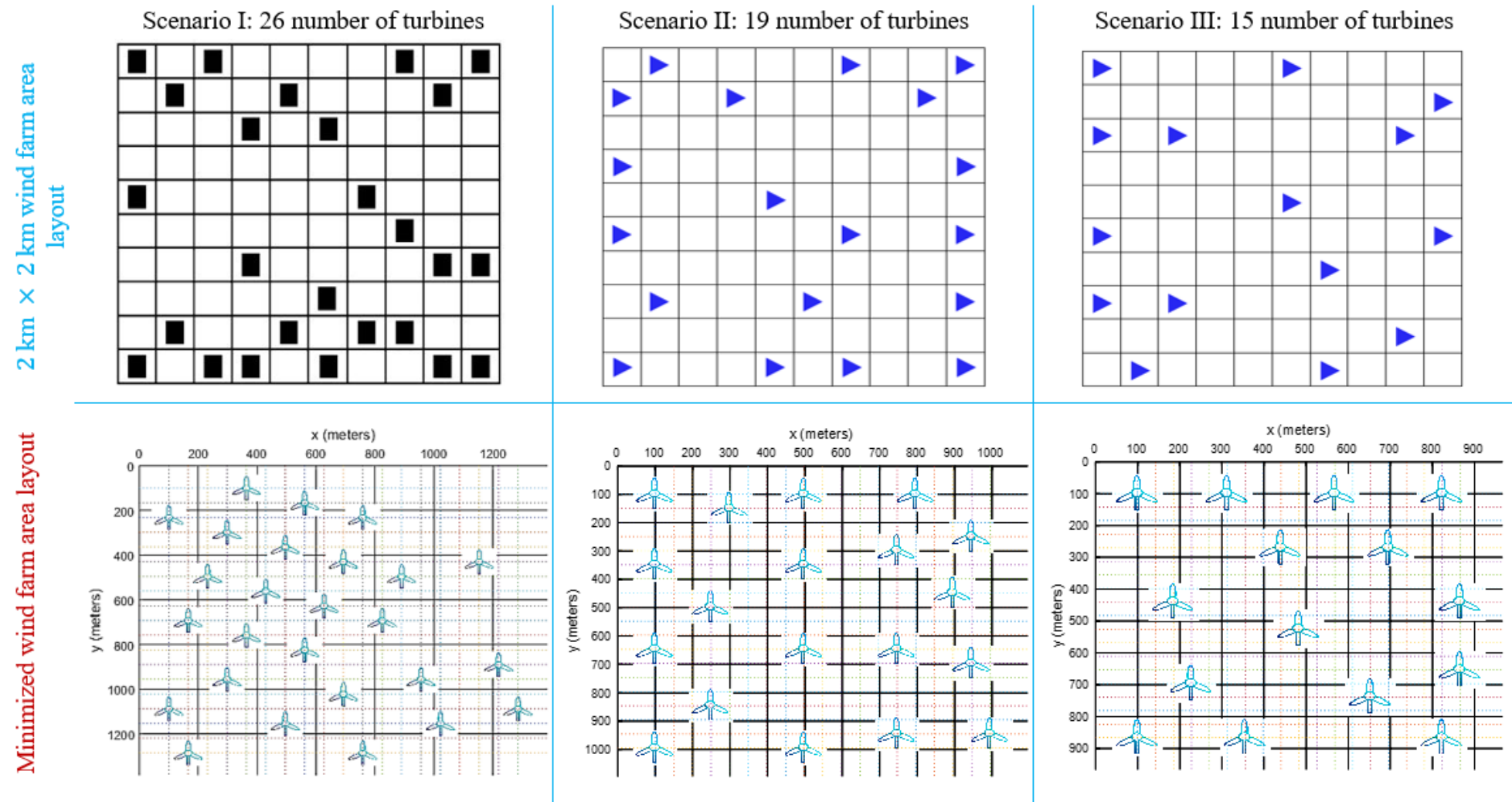


Figure 6. Proposed optimal placements in a minimized land area using Mosetti et al. [1] vs. WFAO-ETLBO.

3.2. Case 2 vs. WFAO–ETLBO

The Case 2 includes the same optimization problems considered by Grady et al. with a fixed land area of $2 \text{ km} \times 2 \text{ km}$, considering 30 turbines for Scenario-I, 39 turbines for Scenario-II, and 39 turbines for Scenario-III for the optimal micro-siting of the wind farm. The results reported by Grady et al. are symmetrical because he optimized only one column and translated the results to all the columns. The symmetrical configuration has an objective function value lower than that of Mosetti et al. [2].

WFAO–ETLBO algorithm is also used to solve the same scenarios considered by Grady et al. Table 2 shows the comparisons of results for all the wind scenarios obtained by Grady et al. and WFAO–ETLBO with fine grid meshing. The total power produced is 2.37%, 1.05%, and 3.02% lower than those quoted by Grady et al. for all the scenarios, respectively. The relative change (R.C.) in efficiency is 2.37%, 1.05%, and 2.65%, respectively, for all the scenarios. From Table 2, it can also be noted that the algorithm is converged in a significantly smaller number of iterations as compared to Grady's. Figure 7 represents difference plots for each learner to ensure the convergence of the WFAO–ETLBO algorithm and show the convergence of the land area for optimal placement of wind turbines in the case of all the scenarios, respectively. The most optimal layouts generated with fine grid meshing for Scenario-I, Scenario-II, and Scenario-III, respectively, are shown in Figure 8, along with the original layouts proposed by Grady et al. The same number of turbines are placed at the optimal locations with a significant reduction of 30.75%, 7.2%, and 7.2% in the land area for Scenario-I, Scenario-II, and Scenario-III, respectively, while producing comparable power for each scenario.

Table 2. Comparisons of results obtained by Grady et al. [2] and WFAO–ETLBO.

	Scenario-I		Scenario-II		Scenario-III	
	Grady et al.	WFAO–ETLBO	Grady et al.	WFAO–ETLBO	Grady et al.	WFAO–ETLBO
Number of turbines	30	30	39	39	39	39
Number of individuals	600	100	600	100	600	100
Fitness value	0.0015436	0.0015812	0.0015666	0.0015800	0.0008403	0.0008665
Total Power (KW/year) (R.C. (%))	14,310	13,969.59 (2.37)	17,220	17,039.24 (1.05)	32,038	31,068.72 (3.02)
Efficiency (%) (R.C. (%))	92.015	89.83 (2.37)	85.174	84.28 (1.05)	86.619	84.32 (2.65)
Converged number of iterations	1203	15	3000	20	1000	30
Area Used (m)	2000×2000	1385×1385	2000×2000	1856×1856	2000×2000	1856×1856
% Reduction in Area	~	30.75	~	7.2	~	7.2
Simulation Time (s)	Not reported	134.86	Not reported	4978.29	Not reported	4101.44

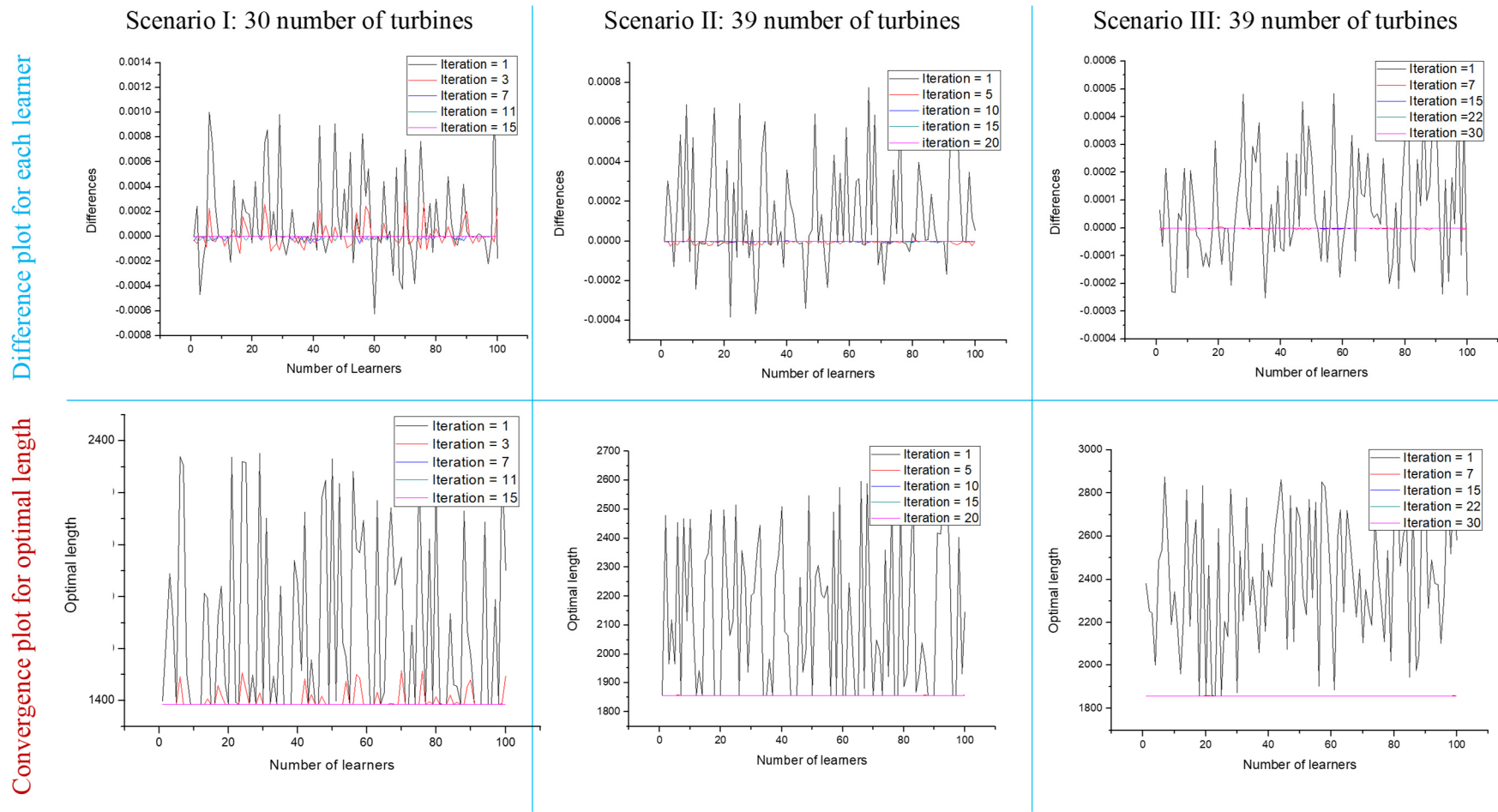
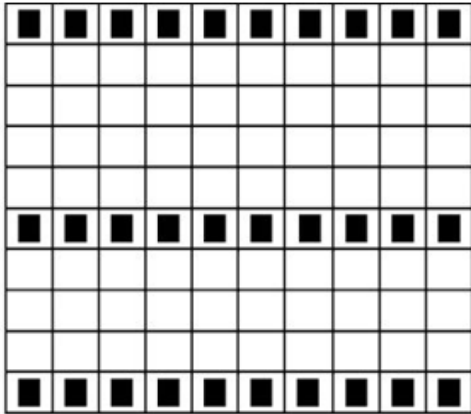


Figure 7. Difference plots for each learner and convergence plots for optimal length for all Scenarios using WFAO–ETLBO.

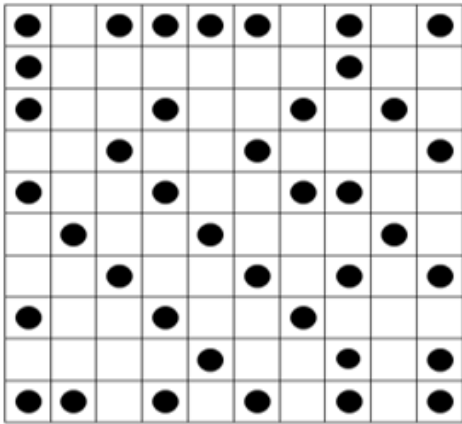
2 km × 2 km wind farm area layout

Minimized wind farm area layout

Scenario I: 30 number of turbines



Scenario II: 39 number of turbines



Scenario III: 39 number of turbines

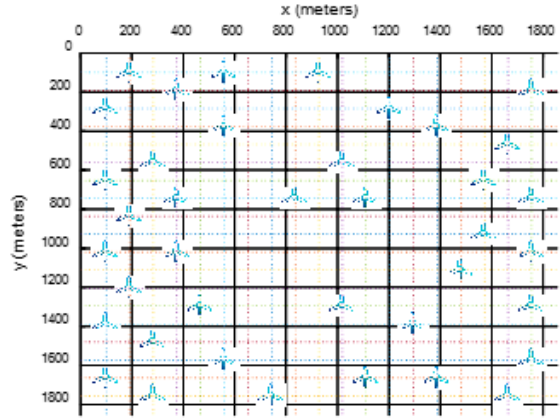
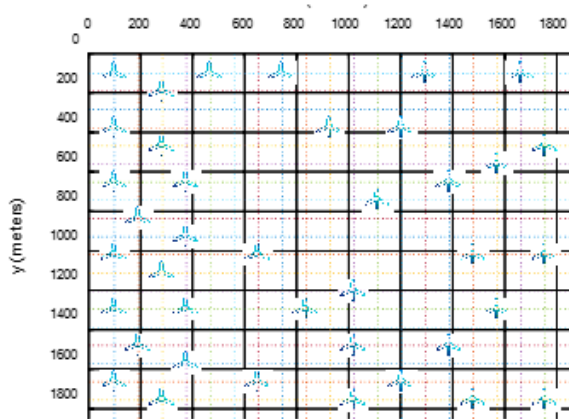
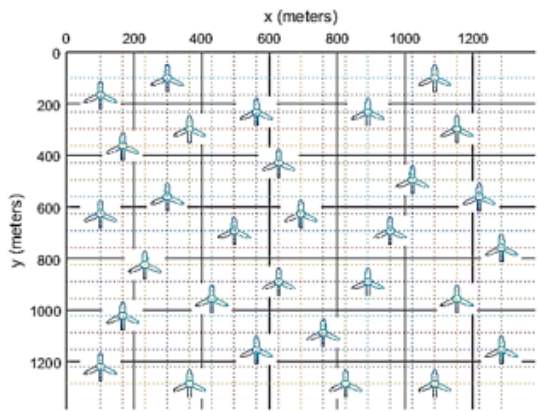
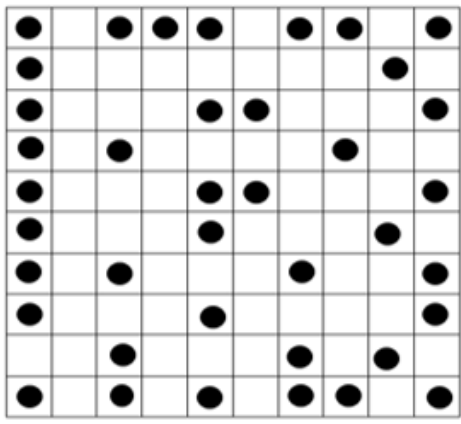


Figure 8. Proposed optimal placements in a minimized land area using Grady et al. [2] vs. WFAO-ETLBO.

3.3. Case 3 vs. WFAO–ETLBO

The Case 3 includes the same wind scenarios considered by Mittal et al. Mittal et al. used 44 fixed turbines for Scenario-I, 38 turbines for Scenario-II, and 41 turbines for Scenario-III placed in a fixed land area of $2 \text{ km} \times 2 \text{ km}$ to find the optimal locations of the wind turbines [3].

WFAO–ETLBO algorithm is finally used to solve the same scenarios considered by Mittal et al. Table 3 shows the comparisons of results for all the wind scenarios obtained by Mittal et al. with those obtained from WFAO–ETLBO with fine grid meshing. The total power produced is 5.36%, 2.71%, and 2.34% lower than those quoted by Mittal et al. for all the scenarios, respectively. The relative change (R.C.) in efficiency is 5.77%, 2.71%, and 3.32%, respectively, for all the scenarios. From Table 3, it can also be noted that the algorithm is converged in a significantly smaller number of iterations as compared to Mittal. Thus, the computational expense of WFAO–ETLBO is expressively very small in comparison with the soft computing technique used in past studies. Figure 9 represents difference plots for each learner to ensure the convergence of the WFAO–ETLBO algorithm and show the convergence of the land area for optimal placement of wind turbines in the case of all the scenarios, respectively. The most optimal layouts generated with fine grid meshing for Scenario-I, Scenario-II, and Scenario-III, respectively, are shown in Figure 10, along with the original layouts proposed by Mittal et al. The same number of turbines are placed at the optimal locations with a significant reduction of 7.2% in the land area for all the scenarios while producing comparable power for each scenario.

Table 3. Comparisons of results obtained by Mittal et al. [3] and WFAO–ETLBO.

	Scenario-I		Scenario-II		Scenario-III	
	Mittal et al.	WFAO–ETLBO	Mittal et al.	WFAO–ETLBO	Mittal et al.	WFAO–ETLBO
Number of turbines	44	44	38	38	41	41
Number of individuals	Not reported	100	Not reported	100	Not reported	100
Fitness value	0.0013602	0.0015101	0.0015273	0.0015699	0.00084379	0.0008641
Total Power (KW/year) (R.C. (%))	21.936	20,758.66 (5.36)	17,259	16,790.89 (2.71)	33,262	32,482.32 (2.34)
Efficiency (%) (R.C. (%))	96.17	90.62 (5.77)	87.612	85.24 (2.71)	86.729	83.85 (3.32)
Converged number of iterations	Not reported	23	Not reported	15	Not reported	20
Area Used (m)	2000×2000	1856×1856	2000×2000	1856×1856	2000×2000	1856×1856
% Reduction in Area	~	7.2	~	7.2	~	7.2
Simulation Time (s)	Not reported	94.51	Not reported	1950.44	Not reported	3002.15

Difference plot for each learner

Convergence plot for optimal length

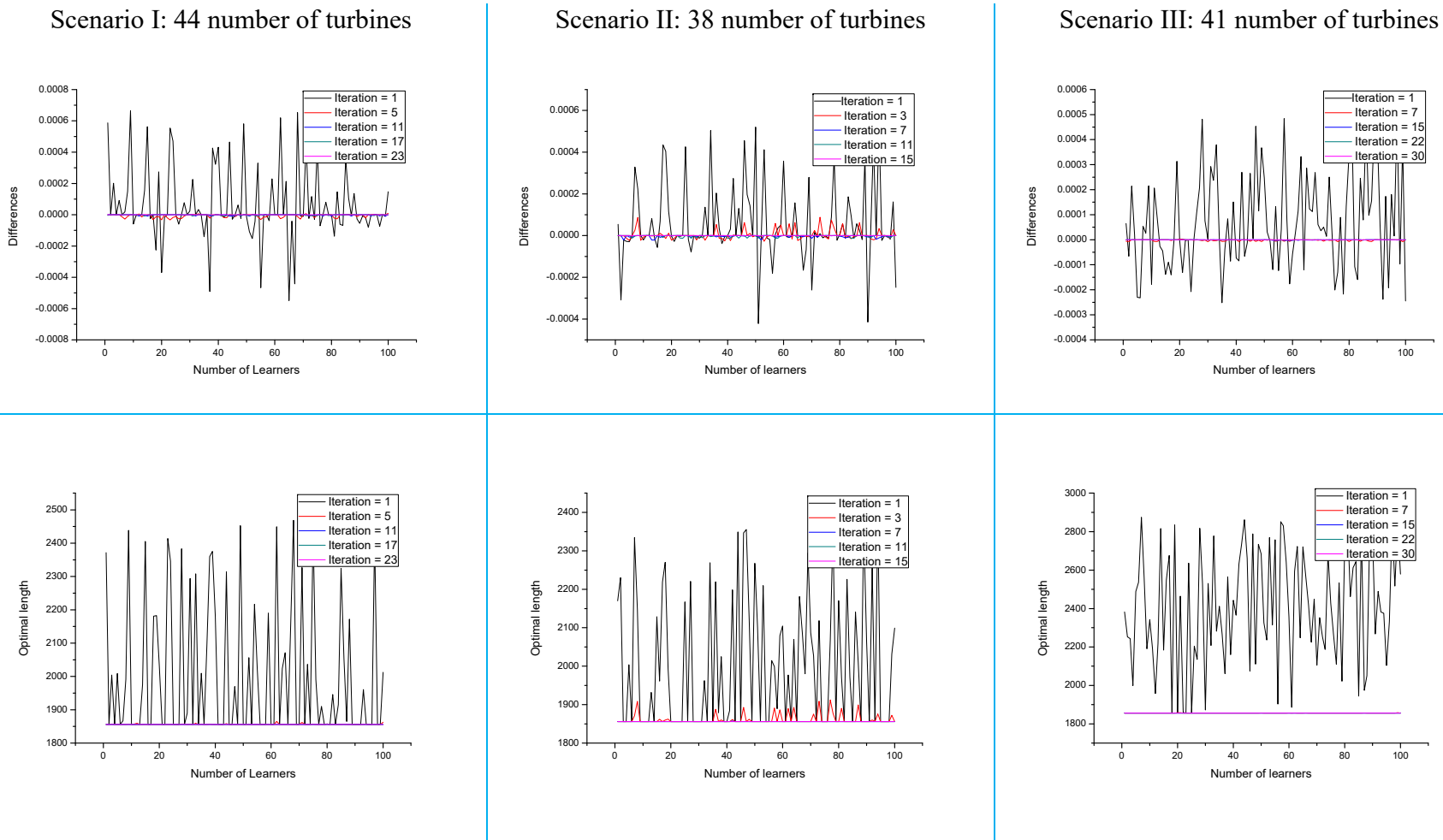
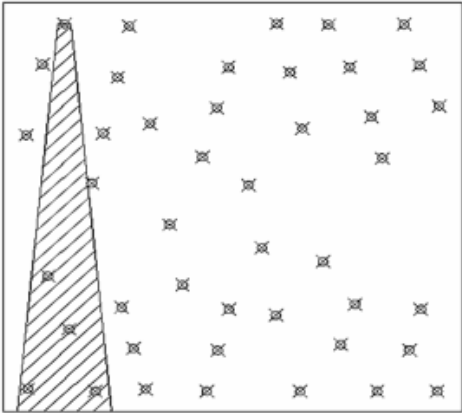


Figure 9. Difference plots for each learner and convergence plots for optimal length for all Scenarios using WFAO-ETLBO.

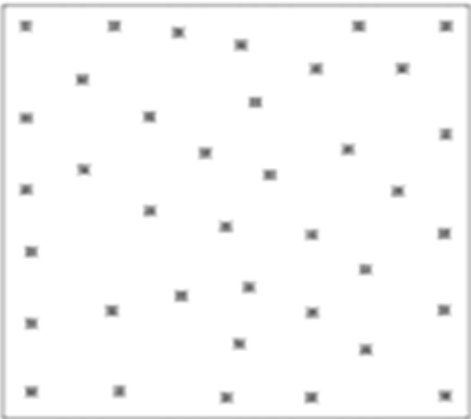
2 km × 2 km wind farm area layout

Minimized wind farm area layout

Scenario I: 44 number of turbines



Scenario II: 38 number of turbines



Scenario III: 41 number of turbines

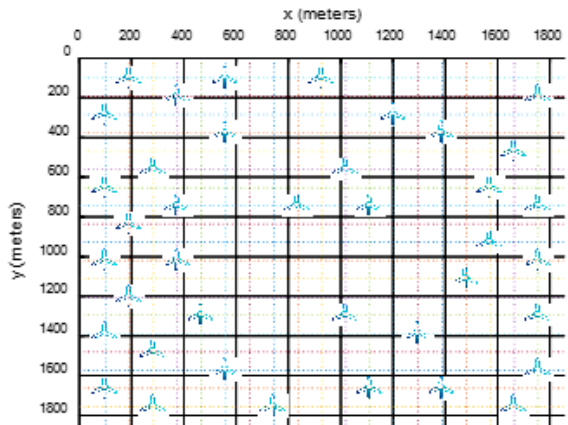
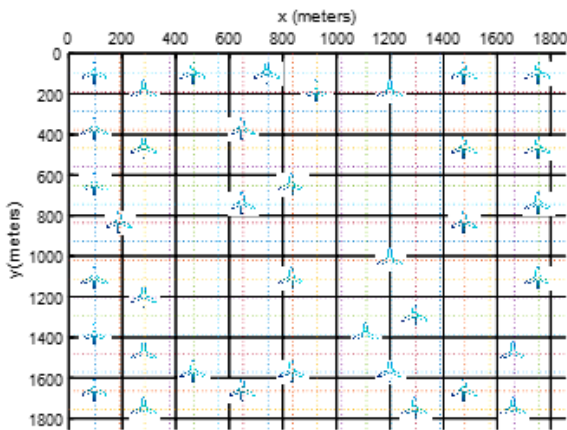
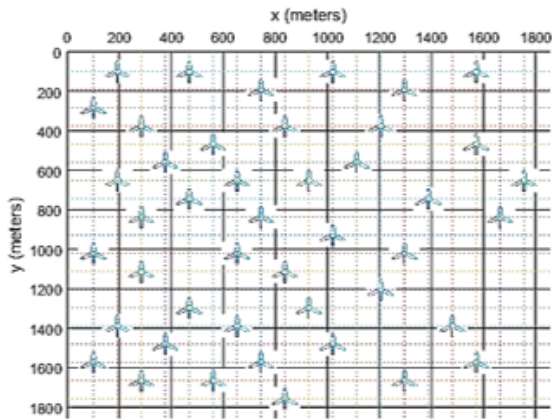
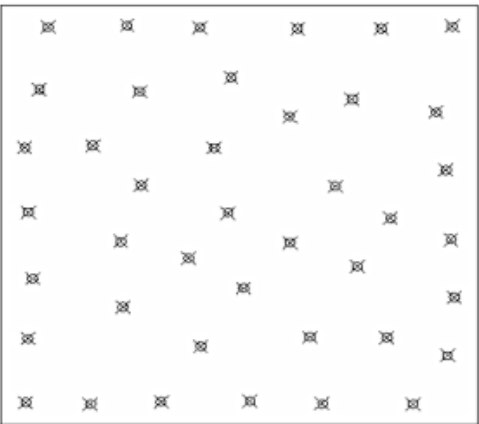


Figure 10. Proposed optimal placements in a minimized land area using Mittal et al. [3] vs. WFAO-ETLB.

In Figure 11 below, it can be observed that the optimum point of efficiency is at 26 turbines for all the nine cases with a different number of turbines used in this study, where efficiency is higher than other approaches, and then it reduces swiftly again, but after 41 turbines it again started to increase. From Figure 12, it can be clearly observed that the optimum point of total power is at 41 turbines for all the nine cases with a different number of turbines used in this study, where total power is higher than other approaches, and then it reduces swiftly again before and after the 41 turbines. It can be concluded that the generalization of the number of turbines is not possible, for which the proposed methodology gives the best result.

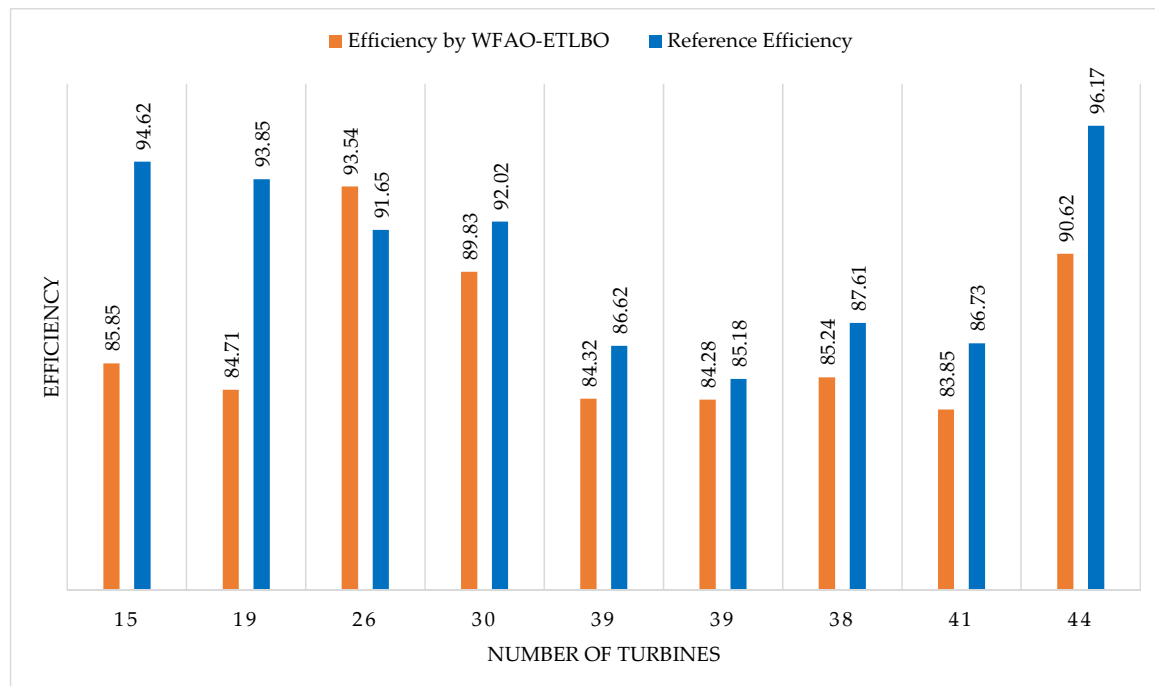


Figure 11. Behaviour of efficiency with increasing number of turbines.

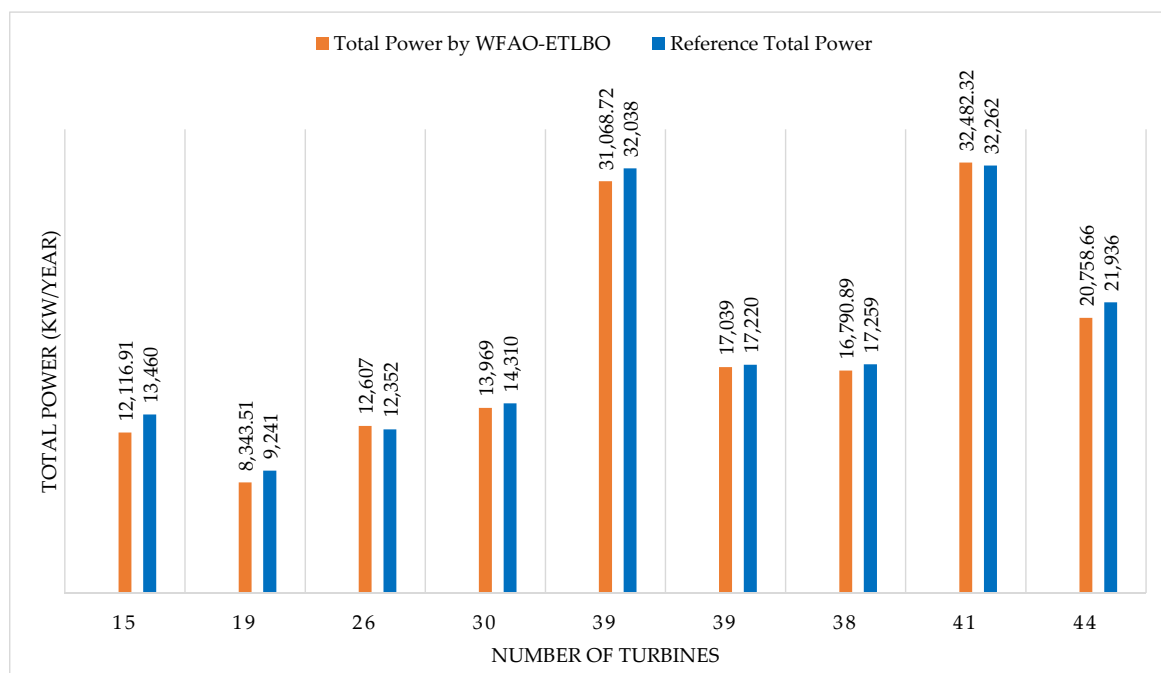


Figure 12. Behaviour of total power with increasing number of turbines.

4. Conclusions

The main objective of this study was to perform Wind Farm Area Optimization (WFAO) for optimal placement of wind turbines using the Elitist Teaching Learning-based Optimization (ETLBO) method. Three different wind scenarios (Scenario-I: fixed wind direction and constant velocity, Scenario-II: variable wind direction and constant velocity, Scenario-III: variable wind direction and variable velocity) were considered in order to minimize the square land area with a fixed number of wind turbines while maximizing the power generation with minimum cost. The results of WFAO–ETLBO have been compared with the results of three researchers who conducted the optimization studies by considering the fixed land area of $2\text{ km} \times 2\text{ km}$. Same wind scenarios have been considered by these three researchers. In the first case (Mosetti et al.), there is a significant reduction in land area for all the scenarios. For Scenario-I, there is an increase of 2.07% in both power and efficiency. While in the case of Scenario-II and Scenario-III, the relative change in power, as well as inefficiency, is 9.74% and 9.26%, respectively, which is less compared to the 45.25% and 51.75% reduction in land area, respectively. In the second case (Grady et al.), there is a significant reduction in land area for Scenario-I as compared to Scenario-II and Scenario-III. For all the three scenarios, the relative change in power, as well as inefficiency, is 2.37%, 1.05%, and 3.02%, respectively, which is again relatively less as compared to the 30.75%, 7.2%, and 7.2% reduction in land area respectively. In the third case (Mittal et al.), there is a reasonable reduction of 7.2% in land area for all the scenarios. The relative change in power, as well as inefficiency, is 5.77%, 2.71%, and 3.32%, respectively, which is again less compared to the 7.2% reduction in land area. Based on the above comparison, the relative reduction in power and efficiency are less than the relative reduction in land area. For all three cases, the ETLBO method has proposed the optimized wind farm layout with a reduced land area with a maximum power output decrease of 9.97% while saving a lot of computational effort.

For design efforts, multiple factors need to be optimized, and each optimization requires significant effort. For example, the third scenario is close to a realistic scenario with variable wind speed and variable direction for which computational cost matters. Therefore, savings in computational efforts of the proposed approach without compromising the design quality is worth mentioning. Therefore, it can be concluded that the ETLBO method can be efficiently applied for wind farm area optimization and for optimal placements of wind turbines with less computational cost as compared to past studies. Another aspect includes the economic advantage of a reduction in land cost due to the reduction in land area with the same number of wind turbines. This impact will be discussed and will be considered in more detail in the upcoming research on the realistic wind farm installed at the Jhampir, Sindh, Pakistan, using more recent and sophisticated wake models along with the new formulations of the objective function by taking into account the available number of turbines and the available budget.

Author Contributions: N.S. and M.A. conceived of the presented idea. M.N.H. and N.S. developed the theory and performed the computations. A.H., A.A., Z.R. and M.A.U.R.T. verified the strategy implemented. M.A.U.R.T. and A.H. encouraged M.N.H. to investigate the teaching–learning based algorithm for the micro-siting of wind turbines in a minimized land area and N.S. supervised the findings of this work. All authors equally contributed in writing the initial and final draft of the manuscript. All authors have read and agreed to the published version of the manuscript.

Funding: This research received no external funding.

Informed Consent Statement: Not applicable.

Data Availability Statement: Not applicable.

Acknowledgments: The authors would like to sincerely appreciate the provision of relevant data by Alternative Energy Development Board (AEDB) in Pakistan.

Conflicts of Interest: The authors declare no conflict of interest.

Nomenclature

WFAO	Wind farm area optimization
ETLBO	Elitist Teaching–Learning-Based Optimization
u_0	undisturbed/freestream wind speed
a	interference coefficient/induction/perturbation coefficient
r_r	rotor radius
r_1	downstream rotor radius
d	rotor diameter
x	wind downstream distance
θ	wake spread angle
α	entrainment constant
K.E.	kinetic energy
N	number of turbines
P	actual power of wind turbine
P_{ideal}	ideal power of wind turbine
ρ	density
u_{wmwe}	velocity of the turbine with multiple wake effect
η	efficiency of wind farm
P_{wmwe}	power with multiple wake effects
P_{wowe}	power without wake effects
L_{mean}	Mean of a learner
$L_{teacher}$	Best learner identified as a teacher
T_F	Teaching factor
$rand$	Uniformly distributed random
L_i	i^{th} learner
L_j	j^{th} learner
$f(L)$	Fitness value of learner
ε	convergence criteria
R.C.	relative change

References

1. Mosetti, G.; Poloni, C.; Diviacco, B. Optimization of wind turbine positioning in large wind farms by means of a genetic algorithm. *J. Wind Eng. Ind. Aerod.* **1994**, *51*, 105–116. [\[CrossRef\]](#)
2. Grady, S.A.; Hussaini, M.Y.; Abdullah, M.M. Placement of wind turbines using genetic algorithms. *Renew. Energy* **2005**, *30*, 259–270. [\[CrossRef\]](#)
3. Mittal, A.; Taylor, L.K. Optimization of Large Wind Farms Using a Genetic Algorithm. In Proceedings of the ASME 2012 International Mechanical Engineering Congress & Exposition, Houston, TX, USA, 9–15 November 2012. [\[CrossRef\]](#)
4. Emami, A.; Noghreh, P. New approach on optimization in placement of wind turbines within wind farm by genetic algorithms. *Renew. Energy* **2010**, *35*, 1559–1564. [\[CrossRef\]](#)
5. Jensen, N.O. *A Note on Wind Generator Interaction*; Technical Report Riso-M-2411; Risø National Laboratory: Roskilde, Denmark, 1983.
6. Shakoor, R.; Hassan, M.Y.; Raheem, A.; Rasheed, N.; Mohd Nasir, M.N. Wind Farm Layout Optimization by Using Definite Point Selection and Genetic Algorithm. In Proceedings of the 2014 IEEE International Conference on Power and Energy (PECon), Kuching, Malaysia, 1–3 December 2014; pp. 191–195.
7. Bastankhah, M.; Porte-Agel, F. A new analytical model for wind-turbine wakes. *Renew. Energy* **2017**, *70*, 116–123. [\[CrossRef\]](#)
8. Kuo, J.Y.J.; Romero, D.A.; Amon, C.H. A mechanistic semi-empirical wake interaction model for wind farm layout optimization. *Energy* **2015**, *93*, 2157–2165. [\[CrossRef\]](#)
9. El-Shorbagy, M.A.; Mousa, A.A.; Nasr, S.M. A chaos-based evolutionary algorithm for general nonlinear programming problems. *Chaos Solit. Fractals* **2016**, *85*, 8–21. [\[CrossRef\]](#)
10. Chen, K.; Song, M.X.; Zhang, X.; Wang, S.F. Wind farm layout optimization using genetic algorithm with different hub height wind turbines. *Renew. Energy* **2016**, *96*, 676–686. [\[CrossRef\]](#)
11. Turner, S.D.O.; Romero, D.A.; Zhang, P.Y.; Amon, C.H.; Chan, T.C.Y. A new mathematical programming approach to optimize wind farm layouts. *Renew. Energy* **2014**, *63*, 674–680. [\[CrossRef\]](#)
12. Ituarte-Villarreal, M.; Espiritu, J.F. Optimization of wind turbine placement using a viral based optimization algorithm. *Procedia Comput. Sci.* **2011**, *6*, 469–474. [\[CrossRef\]](#)
13. Ajit, P.C.; John, C.; Lars, J.; Mahdi, K. Offshore wind farm layout optimization using particle swarm optimization. *J. Ocean. Eng. Mar. Energy* **2018**, *4*, 73–88.

14. Martina, F. Mixed Integer Linear Programming for new trends in wind farm cable routing. *Electron. Notes Dis. Math.* **2018**, *64*, 115–124.
15. Gao, X.; Yang, H.; Lin, L.; Koo, P. Wind turbine layout optimization using multi-population genetic algorithm and a case study in Hong Kong offshore. *J. Wind Eng. Ind. Aerod.* **2015**, *139*, 89–99. [\[CrossRef\]](#)
16. Eroglu, Y.; Seçkiner, S.U. Design of wind farm layout using ant colony algorithm. *Renew. Energy* **2012**, *44*, 53–62. [\[CrossRef\]](#)
17. Feng, J.; Shen, W.Z. Solving the wind farm layout optimization problem using random search algorithm. *Renew. Energy* **2015**, *78*, 182–192. [\[CrossRef\]](#)
18. Feng, J.; Shen, W.Z. Optimization of wind farm layout: A refinement method by random search. In Proceedings of the 2013 International Conference on Aerodynamics of Offshore Wind Energy Systems and Wakes, Copenhagen, Denmark, 17–19 June 2013.
19. Wagner, M.; Day, J.; Neumann, F. A fast and effective local search algorithm for optimizing the placement of wind turbines. *Renewable Energy* **2013**, *51*, 64–70. [\[CrossRef\]](#)
20. Yang, K.; Cho, K. Simulated Annealing Algorithm for Wind Farm Layout Optimization: A Benchmark Study. *Energies* **2019**, *12*, 4403. [\[CrossRef\]](#)
21. Majid, K.; Shahrzad, A.; Mahmoud, O.; Forough, K.N.; Kwok, W.C. Optimizing layout of wind farm turbines using genetic algorithms in Tehran province, Iran. *Int. J. Energy Environ. Eng.* **2018**, *9*, 399–411. [\[CrossRef\]](#)
22. Niayifar, A.; Porté-Agel, F. Analytical Modeling of Wind Farms: A New Approach for Power Prediction. *Energies* **2016**, *9*, 741. [\[CrossRef\]](#)
23. Kusiak, A.; Zhe, S. Design of wind farm layout for maximum wind energy capture. *Renew. Energy* **2010**, *35*, 685–694. [\[CrossRef\]](#)
24. Abdulrahman, M.; Wood, D. Wind Farm Layout Upgrade Optimization. *Energies* **2019**, *12*, 2465. [\[CrossRef\]](#)
25. Roque, P.M.J.; Chowdhury, S.P.; Huan, Z. Performance Enhancement of Proposed Namaacha Wind Farm by Minimising Losses Due to the Wake Effect: A Mozambican Case Study. *Energies* **2021**, *14*, 4291. [\[CrossRef\]](#)
26. Kirchner-Bossi, N.; Porté-Agel, F. Wind Farm Area Shape Optimization Using Newly Developed Multi-Objective Evolutionary Algorithms. *Energies* **2021**, *14*, 4185. [\[CrossRef\]](#)
27. Hsieh, Y.Z.; Lin, S.S.; Chang, E.Y.; Tiong, K.K.; Tan, S.W.; Hor, C.Y.; Cheng, S.C.; Tsai, Y.S.; Chen, C.R. Wind Technologies for Wake Effect Performance in Windfarm Layout Based on Population-Based Optimization Algorithm. *Energies* **2021**, *14*, 4125. [\[CrossRef\]](#)
28. Yeghikian, M.; Ahmadi, A.; Dashti, R.; Esmailion, F.; Mahmoudan, A.; Hoseinzadeh, S.; Garcia, D.A. Wind Farm Layout Optimization with Different Hub Heights in Manjil Wind Farm Using Particle Swarm Optimization. *Appl. Sci.* **2021**, *11*, 9746. [\[CrossRef\]](#)
29. Al-Addous, M.; Jaradat, M.; Albatayneh, A.; Wellmann, J.; Al Hmidan, S. The Significance of Wind Turbines Layout Optimization on the Predicted Farm Energy Yield. *Atmosphere* **2020**, *11*, 117. [\[CrossRef\]](#)
30. Bai, F.; Ju, X.; Wang, S.; Zhou, W.; Liu, F. Wind farm layout optimization using adaptive evolutionary algorithm with Monte Carlo Tree Search reinforcement learning. *Energy Convers. Manag.* **2022**, *15*, 115047. [\[CrossRef\]](#)
31. Zilong, T.; Wei, D.X. Layout optimization of offshore wind farm considering spatially inhomogeneous wave loads. *Appl. Energy* **2022**, *306*, 117947. [\[CrossRef\]](#)
32. Masoudi, S.M.; Baneshi, M. Layout optimization of a wind farm considering grids of various resolutions, wake effect, and realistic wind speed and wind direction data: A techno-economic assessment. *Energy* **2022**, *244*, 123188. [\[CrossRef\]](#)
33. Porté-Agel, F.; Bastankhah, M.; Shamsoddin, S. Wind-Turbine and Wind-Farm Flows: A Review. *Bound. Layer Meteorol.* **2019**, *174*, 1–59. [\[CrossRef\]](#)
34. King, R.N.; Dykes, K.; Graf, P.; Hamlington, P.E. Optimization of wind plant layouts using an adjoint approach. *Wind. Energy Sci.* **2017**, *2*, 115–131. [\[CrossRef\]](#)
35. Antonini, E.G.A.; Romero, D.A.; Amon, C.H. Optimal design of wind farms in complex terrains using computational fluid dynamics and adjoint methods. *Appl. Energy* **2020**, *261*, 114426. [\[CrossRef\]](#)
36. Dhoot, A.; Antonini, E.G.A.; Romero, D.A.; Amon, C.H. Optimizing wind farms layouts for maximum energy production using probabilistic inference: Benchmarking reveals superior computational efficiency and scalability. *Energy* **2021**, *223*, 120035. [\[CrossRef\]](#)
37. Shakoor, R.; Hassan, M.Y.; Raheem, A.; Rasheed, N. Wind farm layout optimization using area dimensions and definite point selection techniques. *Renew. Energy* **2016**, *88*, 154–163. [\[CrossRef\]](#)
38. Rao, R.V. *Teaching-Learning Based Optimization and Its Engineering Applications*; Springer: London, UK, 2015.
39. Ammar, A.; Ahmad, S.I. Teaching-learning based optimization algorithm for core reload pattern optimization of a research reactor. *Ann. Nucl. Energy* **2019**, *133*, 169–177. [\[CrossRef\]](#)
40. Rao, R.V.; Patel, V. An elitist teaching-learning-based optimization algorithm for solving complex constrained optimization problems. *Int. J. Ind. Eng. Comput.* **2012**, *3*, 535–560. [\[CrossRef\]](#)
41. Rao, R.V.; Patel, V. Comparative performance of an elitist teaching-learning based optimization algorithm for solving unconstrained optimization problems. *Int. J. Ind. Eng. Comput.* **2013**, *4*, 29–50. [\[CrossRef\]](#)
42. Rao, R.V.; Savsani, V.J.; Vakharia, D.P. Teaching-learning-based optimization: A novel method for constrained mechanical design optimization problems. *Comput.-Aided Des.* **2011**, *43*, 303–315. [\[CrossRef\]](#)